

Global infrared rearrangements and the renormalisation of QCD

Giulio Falcioni

Hamburg-Nikhef collaboration

K. Chetyrkin, F. Herzog and J. Vermaseren

Based on

JHEP10 (2017) 179, arxiv:1709.08541; To appear

20 Nov 2017 – IIT Hyderabad

Outline

1 Introduction

2 Global IR rearrangements

3 Renormalisation of gauge theories

4 Conclusion and outlook

Motivation

Problem: find the UV counterterm $Z(\gamma)$ of a Feynman diagram γ

Applications:

- Compute the singular part of higher-loop diagrams

$$K_\epsilon(\Gamma) = - \sum_{\substack{\gamma \in \Gamma \\ \gamma \neq \emptyset}} Z(\gamma) * \Gamma/\gamma \quad (1.1)$$

K_ϵ extracts the pole part, Γ/γ is the reduced graph.

- Renormalisation group functions (e.g. anomalous dimensions)

Origin of IR rearrangements

In MS scheme $Z(\gamma)$ is a polynomial in the masses ([Collins, 1977](#)).

- If γ is logarithmically divergent $Z(\gamma)$ is mass-independent.
 γ can always be made log-divergent by taking derivatives.
- *Infrared rearrangements* (IRRs), acting on masses and external momenta, simplify the calculation of $Z(\gamma)$ ([Vladimirov, 1980](#)).

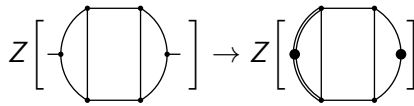
$$Z\left[\begin{array}{c} \text{---} \\ \text{---} \end{array}\right] = Z\left[\begin{array}{c} \text{---} \\ \text{---} \end{array}\right] = Z\left[\begin{array}{c} \text{---} \\ \text{---} \end{array}\right]$$

Double lines are massive propagators, dotted lines are squared propagators.

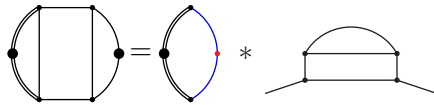
One-mass tadpoles (I)

IRRs reduce the complexity of the calculation of **1 loop**.

- Global IRR applies the same rearrangement to all diagrams.
Ex: **three-loop** propagator

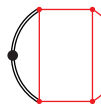


Factorisation into one-loop tadpole and two-loop propagator

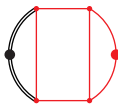


One-mass tadpoles (II)

More in detail


$$\text{Diagram: A loop with a vertical line segment connecting the top and bottom vertices. The left vertex is black, the right is red. A curved line enters from the left, loops around, and exits to the right.} = \int d^d q \frac{1}{[q^2 + M^2]^2} * \Pi(q^2)$$

Dimensional analysis: $\Pi(q^2) = (q^2)^{-2-2\epsilon} \zeta$. In conclusion


$$\text{Diagram: Same as above, but the denominator includes a factor of } (q^2)^{2+2\epsilon}$$
$$= \int d^d q \frac{\zeta}{[q^2 + M^2]^2 (q^2)^{2+2\epsilon}}$$

- IR divergences are generated at $q \rightarrow 0$!

Dealing with IR singularities

IRRs can generate IR poles: we need a strategy to deal with them.

$$\int \frac{d^d q}{(2\pi)^d} \cdots \int \frac{d^d k}{(2\pi)^d} \frac{1}{(q+k)^2 [k^2]^2}$$

- Auxiliary mass regulating the IR (Chetyrkin, Misiak, Munz; van Ritbergen, Larin, Vermaseren '97)
- IR counterterms: apply the R^* operation (Chetyrkin, Smirnov, Tkachov '82, '84-'85)

$$R^*(\Gamma) = \tilde{R} \circ R(\Gamma) \quad (1.2)$$

\tilde{R} recursively subtracts IR divergences from each diagram.

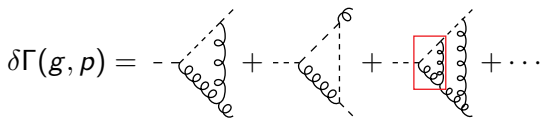
Global approach

The R^* operation is very flexible, because it allows general rearrangements of each Feynman diagram separately.

- IR counterterms must be computed on a diagram-by-diagram basis
- high-order calculation can involve $\mathcal{O}(10^5)$ Feynman diagrams, with many IR counterterms per diagram → **Bottleneck**
- **Global R^*** ([Chetyrkin 1991](#)) avoids this problem by using a single IR counterterm for the whole process.

An example

Renormalisation of the ghost-gluon vertex



The UV vertex divergence is renormalised by Z_1
 $g \rightarrow g_0$ renormalises all the remaining subdivergences.

$$Z_1 + \delta\Gamma(g_0, p) + \delta Z_1 * \delta\Gamma(g_0, p) = \text{finite} \quad (2.3)$$

An example

Renormalisation of the ghost-gluon vertex

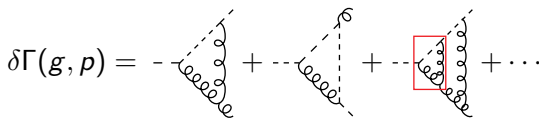
$$\delta\Gamma(g, p) = - \text{---} \circlearrowleft + \text{---} \circlearrowright + \cdots \boxed{\text{---}} \circlearrowleft + \cdots$$

The UV vertex divergence is renormalised by Z_1
 $g \rightarrow g_0$ renormalises all the remaining subdivergences.

$$\delta Z_1 = -K_\epsilon [Z_1 * \delta\Gamma(g_0, p)] \quad (2.3)$$

An example

Renormalisation of the ghost-gluon vertex



The UV vertex divergence is renormalised by Z_1
 $g \rightarrow g_0$ renormalises all the remaining subdivergences.

$$\delta Z_1 = -K_\epsilon \left[Z_1 * \widetilde{R} [\delta\Gamma(p=0)] \right] \quad (2.3)$$

Global R^*

Global infrared rearrangement

We rearrange all the Feynman diagrams into **factorised tadpoles**.

1 Introduction of the mass

$$\delta\Gamma_M(g, p, M) = - \text{---} \circlearrowleft + \cdots \circlearrowleft + \cdots \circlearrowright + \cdots$$

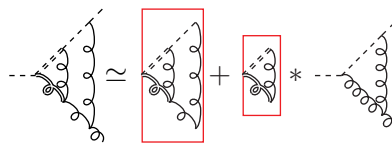
- Vertex divergence (mass independent) renormalises with Z_1
- The **massive vertex** subdivergence changes

$$Z_1 + \delta\Gamma_M(g_0, p, M) + \delta Z_1 * \delta\Gamma(g_0, p) = \text{finite} \quad (2.4)$$

Tadpole Limit

The Feynman integrals approach tadpoles in the limit $M^2 \gg p$.

- 2 Hard mass expansion (Smirnov 1996) expands all the subdiagrams involving heavy lines around $p \rightarrow 0$



In formula

$$\delta\Gamma_M(g_0, p, M) \simeq \boxed{\delta\Gamma_M(g_0, 0, M)} + \boxed{\delta\Gamma_M(g_0, 0, M) * \delta\Gamma(g_0, p, 0)} \quad (2.5)$$

Global infrared counterterm

Z_1 is almost written as one-mass tadpoles.

$\delta\Gamma(g_0, p)$ has IR poles at $p \rightarrow 0$. \tilde{R} can now subtract them at global level.

$$\delta Z_1 = -K_\epsilon \left[\underbrace{\delta\Gamma_M(g_0, 0, M)}_{\text{tadpole}} + \left(\delta\Gamma_M(g_0, 0, M) + \delta Z_1 \right) * \delta\Gamma(g_0, p) \right] \quad (2.6)$$

Global infrared counterterm

Z_1 is almost written as one-mass tadpoles.

$\delta\Gamma(g_0, p)$ has IR poles at $p \rightarrow 0$. \widetilde{R} can now subtract them at global level.

$$\delta Z_1 = -K_\epsilon \left[\underbrace{\delta\Gamma_M(g_0, 0, M)}_{\text{tadpole}} + \left(\delta\Gamma_M(g_0, 0, M) + \delta Z_1 \right) \widetilde{R} \left[\delta\Gamma(g_0, p=0) \right] \right] \quad (2.6)$$

Global infrared counterterm

Z_1 is almost written as one-mass tadpoles.

$\delta\Gamma(g_0, p)$ has IR poles at $p \rightarrow 0$. \tilde{R} can now subtract them at global level.

$$\delta Z_1 = -K_\epsilon \left[\underbrace{\delta\Gamma_M(g_0, 0, M)}_{\text{tadpole}} + \left(\delta\Gamma_M(g_0, 0, M) + \delta Z_1 \right) \tilde{R} \left[\delta\Gamma(g_0, p=0) \right] \right] \quad (2.6)$$

$\tilde{R} \left[\delta\Gamma(p=0) \right]$ is imposed by multiplicative renormalisation

$$\delta Z_1 = -Z_1 * \tilde{R} \left[\delta\Gamma(g_0, p=0) \right]$$

(2.7)

Global R^* at work

- 1 Renormalisation of the globally rearranged diagrams gives

$$\delta Z_1 = -K_\epsilon \left[\delta\Gamma_M(0, M) + (\delta\Gamma_M(0, M) + \delta Z_1) * \tilde{R}[\delta\Gamma(p=0)] \right]$$

Global R^* at work

- 1 Renormalisation of the globally rearranged diagrams gives

$$\delta Z_1 = -K_\epsilon \left[\delta\Gamma_M(0, M) + (\delta\Gamma_M(0, M) + \delta Z_1) * \tilde{R}[\delta\Gamma(p=0)] \right]$$

- 2 introduction of the IR counterterm $\tilde{R}[\delta\Gamma(p=0)]$

$$\tilde{R}[\delta\Gamma(p=0)] = -\frac{\delta Z_1}{Z_1}.$$

Global R^* at work

- 1 Renormalisation of the globally rearranged diagrams gives

$$\delta Z_1 = -K_\epsilon \left[\delta\Gamma_M(0, M) + (\delta\Gamma_M(0, M) + \delta Z_1) * \tilde{R}[\delta\Gamma(p=0)] \right]$$

- 2 introduction of the IR counterterm $\tilde{R}[\delta\Gamma(p=0)]$

$$\tilde{R}[\delta\Gamma(p=0)] = -\frac{\delta Z_1}{Z_1}.$$

- 3 In conclusion Z_1 is determined

$$\delta Z_1 = -K_\epsilon \left[\frac{\delta\Gamma_M(g_0, 0, M)}{Z_1} - \frac{(\delta Z_1)^2}{Z_1} \right] \quad (2.8)$$

Towards 5-loop renormalisation

$$\delta Z_1 = -K_\epsilon \left[\frac{\delta \Gamma_M(g_0, 0, M)}{Z_1} - \frac{(\delta Z_1)^2}{Z_1} \right] \quad (3.9)$$



Counterterms from lower orders.

- We reduced the calculations to factorized L -loop tadpoles.
- We automated the computation of factorized tadpoles using **FORCER** (Ruijl, Ueda, Vermaseren 2017) and determined Z_1 to 5 loops.

Highly efficient approach

Renormalisation of QCD

- The ghost-gluon vertex renormalisation constant Z_1 is the first necessary ingredient to renormalise QCD.
- One of the possible choices includes
 - The ghost field renormalisation Z_3^c
 - The gluon field renormalisation Z_3
 - The quark field renormalisation Z_2
- Ward identities fix the remaining constants

$$Z_g = \frac{Z_1}{Z_3^c \sqrt{Z_3}} = \frac{Z_1^{qqg}}{Z_2 \sqrt{Z_3}} = \frac{Z_1^{3g}}{(Z_3)^{\frac{3}{2}}} \quad (3.10)$$

The ghost field renormalisation

- Let's consider now the global rearrangement for the ghost field

$$\Pi(q^2) = \text{---} \circlearrowleft \text{---} \rightarrow K_\epsilon \left[Z_3^c \left(1 + \Pi(g_0, q^2) \right) \right] = 0$$

$$\Pi(q^2) = \text{---} \circlearrowleft \text{---} \rightarrow K_\epsilon \left[Z_3^c \left(1 + \frac{\Pi_M(q^2, M^2) + \delta Z_1 \cdot \Pi(q^2)}{Z_1} \right) \right] = 0$$

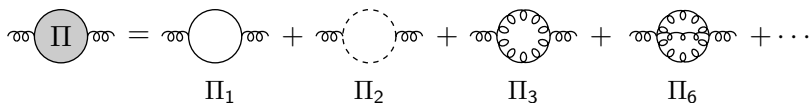
- Using the hard mass expansion and the IR counterterm

$$\delta Z_3^c = -K_\epsilon \left[\frac{Z_3^c}{Z_1} \left(\Pi_M(0, M) - \frac{\delta Z_3^c}{Z_3^c} \left(\delta \Gamma_M(0, M) + \delta Z_1 \right) \right) \right].$$

The gluon field renormalisation

- The gluon renormalisation Z_3 is complicate: first time undertaken in 2016 for $SU(3)$ (Baikov, Chetyrkin, Kühn).

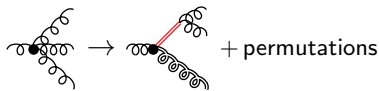
$$K_\epsilon \left[Z_3 \left(1 + \sum_{i=1,2,3,6} \Pi_i(g_0, q) \right) \right] = 0, \quad (3.11)$$



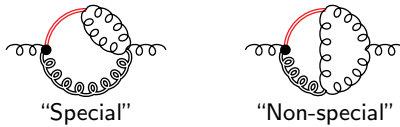
- (a) New rearrangements of 4-point vertices.
- (b) External gluons have many interactions.

Some problems (a)

- Mass insertion in the 4-gluon vertex via an auxiliary field



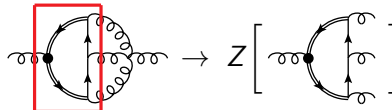
- New “special”, self-energy-like, subdivergences



Some problems (b)

Highly non-trivial renormalisation of the modified vertices:

- vertices mix among each other. *E.g.*



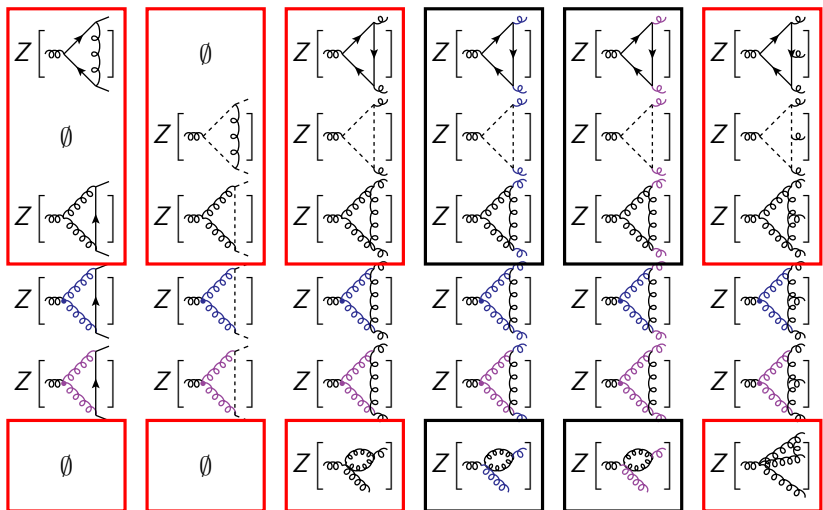
counterterm mixing quark
and 4-gluon operators.

- Mixing into new operators (not in the QCD Lagrangian).
We analysed the operators appearing for **general gauge group**
 - Two new 3-gluon vertices

$$O_4 = \text{---} \quad O_5 = \text{---}$$

- New 4-gluon vertices appear at each loop order: we selected a basis of six new vertices O_7, \dots, O_{12} needed to this order. Note that each of them is splitted with the auxiliary field.

A 12x12 mixing matrix



Solution

Only a small subset of the matrix elements z_{ij} contributes and

$$\sum_{i=1,2,3,6} z_{ij} = \begin{cases} 0, & \text{if } j \in \{4, 5, 7, \dots, 12\} \text{ is a gauge variant operator} \\ Z_1^j, & \text{if } j \in \{1, 2, 3, 6\} \text{ is a QCD operator} \end{cases}$$

where $Z_1^j \in \{Z_1^{ccg}, Z_1^{qqg}, Z_1^{ggg}, Z_1^{gggg}\}$ are QCD vertex renormalisation constant.

Solution

Only a small subset of the matrix elements z_{ij} contributes and

$$\sum_{i=1,2,3,6} z_{ij} = \begin{cases} 0, & \text{if } j \in \{4, 5, 7, \dots, 12\} \text{ is a gauge variant operator} \\ Z_1^j, & \text{if } j \in \{1, 2, 3, 6\} \text{ is a QCD operator} \end{cases}$$

where $Z_1^j \in \{Z_1^{ccg}, Z_1^{qqg}, Z_1^{ggg}, Z_1^{gggg}\}$ are QCD vertex renormalisation constant.

Exploiting these features we write the gluon renormalisation constant in terms of factorized tadpoles $\Pi_i(M)$ and lower order counterterms

$$\begin{aligned} \delta Z_3 &= -K_\epsilon \left\{ \sqrt{Z_3} \sum_{i=1,2,3,6} \left\{ \sum_{j,k} \left[z_{ij}^{sp} \mathbf{Z}_j \left(\Pi_j(M) + \delta \Gamma_{jk}^{ns} \Pi_k(q) \right) \right] \right. \right. \\ &\quad \left. \left. + (\sqrt{Z_3} - \mathbf{Z}_i) \Pi_i(q) - \sum_j \delta z_{ij}^{sp} \mathbf{Z}_j \Pi_j(q) \right\} \right\}. \end{aligned}$$

Results

- Z_1^{ccg} , Z_1^{qqg} , Z_2 , Z_3^c to 5 loops with all the powers of the gauge parameter ξ .
 - Verified $Z_1^{ccg} \propto (1 - \xi)$.
 - Verified consistency with the Ward identities.
- Z_3 to 5 loops, retaining linear terms in ξ .
- We computed the coupling renormalisation

$$Z_\alpha = \frac{(Z_1^{ccg})^2}{Z_3(Z_3^c)^2}, \quad (4.12)$$

- Verified independence on ξ to first order.

Complete renormalisation of QCD to 5 loops in covariant gauges
for general gauge group.

Landau gauge quark anomalous dimension

$$\begin{aligned}
 (\gamma_2)_4 &= C_F \frac{d_A^{abcd} d_A^{abcd}}{N_A} \left[-\frac{1985}{24} + \frac{781753}{192} \zeta_7 - \frac{1458845}{384} \zeta_5 + \frac{135731}{192} \zeta_3 + \frac{3577}{64} \zeta_3^2 \right] \\
 &\quad + T_R \eta_F^4 \frac{d_R^{abcd} d_A^{abcd}}{N_R} \left[\frac{6200}{9} - \frac{1425}{4} \zeta_6 + \frac{27377}{6} \zeta_7 + \frac{1113}{4} \zeta_4 - \frac{9915}{2} \zeta_5 \right. \\
 &\quad \left. - \frac{2468}{3} \zeta_3 + \frac{91}{2} \zeta_3^2 \right] + T_R \eta_F^2 \frac{d_R^{abcd} d_R^{abcd}}{N_R} \left[-\frac{7360}{9} + 640 \zeta_5 + \frac{704}{3} \zeta_3 \right] \\
 &\quad + C_F \eta_F^4 T_R^4 \left[\frac{1328}{243} - \frac{256}{27} \zeta_3 \right] + C_F \frac{d_R^{abcd} d_A^{abcd}}{N_R} \left[\frac{113}{6} - \frac{125447}{8} \zeta_7 \right. \\
 &\quad \left. + 1015 \zeta_5 + 17554 \zeta_3 - 4884 \zeta_3^2 \right] + C_F \eta_F^4 \frac{d_R^{abcd} d_R^{abcd}}{N_R} \left[-\frac{5984}{3} - 8680 \zeta_7 \right. \\
 &\quad \left. + 18080 \zeta_5 - 12096 \zeta_3 + 3648 \zeta_3^2 \right] + C_F^2 \eta_F^3 T_R^3 \left[-\frac{2636}{243} - 64 \zeta_4 + \frac{832}{9} \zeta_3 \right] \\
 &\quad + C_F^3 \eta_F^2 T_R^2 \left[-\frac{2497}{27} - 128 \zeta_4 + 320 \zeta_5 + \frac{400}{9} \zeta_3 \right] + C_F^4 \eta_F T_R \left[\frac{29209}{36} \right. \\
 &\quad \left. + \frac{6400}{3} \zeta_6 - 800 \zeta_4 - \frac{46880}{9} \zeta_5 + \frac{22496}{9} \zeta_3 + \frac{1024}{3} \zeta_3^2 \right] + C_F^5 \left[\frac{4977}{8} \right. \\
 &\quad \left. - 47628 \zeta_7 + 22600 \zeta_5 + 16000 \zeta_3 + 2496 \zeta_3^2 \right]
 \end{aligned}$$

$$\begin{aligned}
& + C_A \frac{d_R^{abcd} d_A^{abcd}}{N_R} \left[-\frac{173959}{144} + \frac{15675}{16} \zeta_6 + \frac{3016307}{256} \zeta_7 - \frac{12243}{16} \zeta_4 \right. \\
& \quad \left. + \frac{609425}{96} \zeta_5 - \frac{574393}{32} \zeta_3 + \frac{16935}{4} \zeta_3^2 \right] \\
& + C_A \eta_F \frac{d_R^{abcd} d_R^{abcd}}{N_R} \left[\frac{33464}{9} + \frac{23632}{3} \zeta_7 - \frac{48640}{3} \zeta_5 + 8992 \zeta_3 - 2320 \zeta_3^2 \right] \\
& + C_A C_F \eta_F^3 T_R^3 \left[-\frac{3566}{243} + 64 \zeta_4 - \frac{1984}{27} \zeta_3 \right] + C_A C_F^2 \eta_F^2 T_R^2 \left[\frac{101485}{162} \right. \\
& \quad \left. + \frac{1600}{3} \zeta_6 + 176 \zeta_4 - \frac{3712}{3} \zeta_5 - \frac{6160}{9} \zeta_3 + \frac{256}{3} \zeta_3^2 \right] + C_A C_F^3 \eta_F T_R \left[-\frac{167263}{108} \right. \\
& \quad \left. - 4800 \zeta_6 - 13944 \zeta_7 + 2120 \zeta_4 + \frac{58720}{3} \zeta_5 - \frac{25804}{9} \zeta_3 - 64 \zeta_3^2 \right] \\
& + C_A C_F^4 \left[-\frac{835739}{144} - \frac{17600}{3} \zeta_6 + 123977 \zeta_7 + 2200 \zeta_4 - \frac{248960}{9} \zeta_5 - \frac{530884}{9} \zeta_3 \right. \\
& \quad \left. - \frac{24632}{3} \zeta_3^2 \right] + C_A^2 C_F \eta_F^2 T_R^2 \left[\frac{120037}{162} - \frac{800}{3} \zeta_6 - \frac{441}{2} \zeta_7 - 179 \zeta_4 + \frac{3584}{9} \zeta_5 \right. \\
& \quad \left. + \frac{3140}{3} \zeta_3 - \frac{128}{3} \zeta_3^2 \right] + C_A^2 C_F^2 \eta_F T_R \left[\frac{717409}{432} + 1150 \zeta_6 + \frac{42203}{3} \zeta_7 - \frac{1411}{4} \zeta_4 \right. \\
& \quad \left. - \frac{95792}{9} \zeta_5 - \frac{14287}{24} \zeta_3 - 1214 \zeta_3^2 \right] + C_A^2 C_F^3 \left[\frac{827215}{72} + 13200 \zeta_6 - \frac{1789067}{16} \zeta_7 \right. \\
& \quad \left. - 4664 \zeta_4 - \frac{188795}{12} \zeta_5 + \frac{1365227}{18} \zeta_3 + \frac{18097}{2} \zeta_3^2 \right] + C_A^3 C_F \eta_F T_R \left[-\frac{31919039}{776} \right. \\
& \quad \left. + \frac{4825}{16} \zeta_6 - \frac{440419}{144} \zeta_7 - \frac{8705}{32} \zeta_4 + \frac{28721}{18} \zeta_5 - \frac{144377}{864} \zeta_3 + \frac{4067}{6} \zeta_3^2 \right]
\end{aligned}$$



$$\begin{aligned}
 & + C_A^3 C_F^2 \left[-\frac{42214139}{3888} - \frac{43175}{6} \zeta_6 + \frac{9074513}{192} \zeta_7 + \frac{3815}{4} \zeta_4 + \frac{5957573}{288} \zeta_5 \right. \\
 & - \frac{5503507}{144} \zeta_3 - \frac{78041}{24} \zeta_3^2 \Big] + C_A^4 C_F \left[\frac{368712343}{62208} + \frac{227975}{192} \zeta_6 \right. \\
 & \left. - \frac{312820991}{36864} \zeta_7 + \frac{87067}{128} \zeta_4 - \frac{16237513}{3072} \zeta_5 + \frac{46196783}{6912} \zeta_3 + \frac{23555}{128} \zeta_3^2 \right].
 \end{aligned}$$

- More complicated structure compared to the beta-function:
 - zeta-values up to weight 7.
- The leading and next-to-leading n_f terms agree with the all-order results of ([Ciuchini et al. '99](#)).

Outlook

- The global R^* method is highly efficient from the computational point of view.
- On the other hand, it is process-dependent → difficult to generalize and automate.
- We tackled the rearrangement of different operators → case study for more applications:
- Determination of the moments of the $N4LO$ splitting functions, whose calculation was shown to be highly demanding.

Thank you